

# Prioritizing bona fide bacterial small RNAs with machine learning classifiers

Erik JJ Eppenhof<sup>1</sup>, Lourdes Peña-Castillo<sup>Corresp. 2,3</sup>

<sup>1</sup> Department of Artificial Intelligence, Radboud University Nijmegen, Nijmegen, Netherlands

<sup>2</sup> Department of Biology, Memorial University of Newfoundland, St. John's, Canada

<sup>3</sup> Department of Computer Science, Memorial University of Newfoundland, St. John's, Canada

Corresponding Author: Lourdes Peña-Castillo

Email address: lourdes@mun.ca

Bacterial small (sRNAs) are involved in the control of several cellular processes. Hundreds of putative sRNAs have been identified in many bacterial species through RNA sequencing. The existence of putative sRNAs is usually validated by Northern blot analysis. However, the large amount of novel putative sRNAs reported in the literature makes it impractical to validate each of them in the wet lab. In this work, we applied five machine learning approaches to construct twenty models to discriminate bona fide sRNAs from random genomic sequences in five bacterial species. Sequences were represented using seven features including free energy of their predicted secondary structure, their distances to the closest predicted promoter site and Rho-independent terminator, and their distance to the closest open reading frames (ORFs). To automatically calculate these features, we developed an sRNA Characterization Pipeline (sRNACharP). All seven features used in the classification task contributed positively to the performance of the predictive models. The best performing model obtained a median precision of 100% at 10% recall and of 64% at 40% recall across all five bacterial species, and it outperformed or was comparable to previous approaches on two benchmark datasets. Our results suggest that even though there is limited sRNA sequence conservation across different bacterial species, there are intrinsic features in the genomic context of sRNAs that are conserved across taxa. We show that these features are utilized by machine learning approaches to learn a species-independent model to prioritize bona fide bacterial sRNAs.

# Prioritizing bona fide bacterial small RNAs with machine learning classifiers

Erik JJ Eppenhof<sup>1</sup> and Lourdes Peña-Castillo<sup>2</sup>

<sup>1</sup>Department of Artificial Intelligence, Radboud University, Nijmegen, GE, The Netherlands

<sup>2</sup>Department of Computer Science and Department of Biology, Memorial University of Newfoundland, St. John's, NL, Canada

Corresponding author:

Lourdes Peña-Castillo<sup>2</sup>

Email address: lourdes@mun.ca

## ABSTRACT

Bacterial small (sRNAs) are involved in the control of several cellular processes. Hundreds of putative sRNAs have been identified in many bacterial species through RNA sequencing. The existence of putative sRNAs is usually validated by Northern blot analysis. However, the large amount of novel putative sRNAs reported in the literature makes it impractical to validate each of them in the wet lab. In this work, we applied five machine learning approaches to construct twenty models to discriminate bona fide sRNAs from random genomic sequences in five bacterial species. Sequences were represented using seven features including free energy of their predicted secondary structure, their distances to the closest predicted promoter site and Rho-independent terminator, and their distance to the closest open reading frames (ORFs). To automatically calculate these features, we developed an sRNA Characterization Pipeline (sRNACHarP). All seven features used in the classification task contributed positively to the performance of the predictive models. The best performing model obtained a median precision of 100% at 10% recall and of 64% at 40% recall across all five bacterial species, and it outperformed or was comparable to previous approaches on two benchmark datasets. Our results suggest that even though there is limited sRNA sequence conservation across different bacterial species, there are intrinsic features in the genomic context of sRNAs that are conserved across taxa. We show that these features are utilized by machine learning approaches to learn a species-independent model to prioritize bona fide bacterial sRNAs.

## INTRODUCTION

Bacterial small RNAs (sRNAs) are ubiquitous regulators of gene expression, mostly acting by antisense mechanisms on multiple target mRNAs and, as a result of this, they are involved in the control of many processes such as adaptive responses, stress responses, virulence, and pathogenicity (Storz et al., 2011; Michaux et al., 2014). Numerous (hundreds) putative sRNAs have been identified in many bacterial species through RNA sequencing (RNA-seq) (e.g., Gröll et al. (2017); Thomason et al. (2015); Zeng and Sundin (2014); McClure et al. (2014)). The existence of putative sRNAs is usually validated by Northern blot analysis. However, the large amount of novel putative sRNAs reported in the literature makes it impractical to validate in the wet lab each of them. To optimize resources, one would like to first investigate those putative sRNAs which are more likely to be bona fide sRNAs. To do that, we need to computationally prioritize sRNAs based on their likelihood of being bona fide sRNAs. Computational prediction of sRNAs in genomic sequences remains a challenging problem, even though tools to tackle this problem have been around since early 2000s (Lu et al., 2011; Backofen and Hess, 2010). Available tools typically use comparative genomics, primary sequence and secondary structure features to predict whether a genomic sequence corresponds to an sRNA, with the comparative genomics-based prediction of sRNAs being the standard method (Lu et al., 2011; Backofen and Hess, 2010). As there are many species-specific sRNAs, and functionally equivalent sRNAs show very low sequence conservation (Wagner and Romby, 2015), a comparative genomics-based model for sRNA prediction (as used by most tools) is not suitable for the majority of sRNAs and many sRNAs are excluded from these predictions. Additionally, as very

48 limited overlap between sRNAs detected by RNA-seq and sRNAs predicted by bioinformatics tools has  
49 been observed in several studies (Soutourina et al., 2013; Wilms et al., 2012; Vockenhuber et al., 2011),  
50 available tools are not suitable for quantifying the probability of a putative sRNA detected from RNA-seq  
51 data being indeed a genuine sRNA. A machine learning-based approach using genomic context features  
52 for sRNA prioritization may be able to overcome the issues caused by the limited sequence conservation  
53 of most sRNAs, and to detect intrinsic features of sRNA sequences common to a number of bacterial  
54 species.

55 The main goal of this study was to develop a bioinformatics tool (applicable to a wide range of  
56 bacterial species) to allow microbiologists to prioritize sRNAs detected from RNA-seq data based on  
57 their probability of being bona fide sRNAs. To do this, we comparatively assessed the performance  
58 of five machine learning approaches for quantifying the probability of a genomic sequence encoding a  
59 bona fide sRNA. The machine learning approaches applied were: logistic regression (LR), multilayer  
60 perceptron (MP), random forest (RF), adaptive boosting (AB) and gradient boosting (GB). We used data  
61 from five bacterial species including representatives from the phyla *Firmicutes* (*Streptococcus pyogenes*),  
62 *Actinobacteria* (*Mycobacterium tuberculosis*), and *Proteobacteria* (*Escherichia coli*, *Salmonella enterica*,  
63 and *Rhodobacter capsulatus*). To assess the applicability of the methods to a wide range of bacteria, we  
64 evaluated the methods in bacterial species not included in the training data. As input to the machine  
65 learning approaches, we provided a vector of seven features per sequence. These features are: the free  
66 energy of the predicted secondary structure, distance to their closest predicted promoter site, distance to  
67 their closest predicted Rho-independent terminator, distances to their two closest open reading frames  
68 (ORFs), and whether or not the sRNA is transcribed on the same strand as their two closest ORFs. These  
69 features were selected under the assumption that genomic context and secondary structure of sRNAs  
70 are better preserved across diverse bacteria than sequence characteristics such as frequencies of mono-  
71 nucleotides, di-nucleotides, and tri-nucleotides. We tested our best performing model in a multi-species  
72 dataset (Lu et al., 2011) and the performance achieved by our method (sRNARanking) demonstrated that  
73 it is possible to create a highly accurate and general (i.e., species-independent) model for prioritizing bona  
74 fide bacterial sRNAs using genomic context features.

75 Obtaining the selected sRNA features requires the use of numerous different bioinformatics tools  
76 which may be challenging for the average user. To facilitate sRNA characterization, we have developed  
77 sRNACharP (sRNA Characterization Pipeline), a pipeline to automatically compute the seven fea-  
78 tures used by sRNARanking (available at <https://github.com/BioinformaticsLabAtMUN/sRNACharP>).  
79 To enable other researchers to use sRNARanking, we made an R script available con-  
80 taining the model (<https://github.com/BioinformaticsLabAtMUN/sRNARanking>). We  
81 expect that together these two tools (sRNACharP and sRNARanking) will facilitate and accelerate the  
82 characterization and prioritization of putative sRNAs helping researchers in the field of RNA-based  
83 regulation in bacteria to focus in the putative sRNAs most likely to be bona fide sRNAs.

## 84 METHODS

### 85 Datasets

86 Published positive instances of bona fide sRNAs were collected for *R. capsulatus* (Grüll et al., 2017),  
87 *M. tuberculosis* (Miotto et al., 2012), *S. pyogenes* (Le Rhun et al., 2016), and *S. enterica* (Kröger et al.,  
88 2012). *M. tuberculosis*, *S. pyogenes* and *S. enterica* positive instances have all been verified by Northern  
89 blot analysis; while, *R. capsulatus* positive instances included, in addition to four experimentally verified  
90 sRNAs, 41 homologous sRNAs (i.e., sRNAs that have high sequence similarity to known sRNAs in other  
91 bacterial species or were found to be conserved in the genome of at least two other bacterial species).  
92 Additionally, we collected *E. coli* sRNAs, supported by literature with experimental evidence from  
93 RegulonDB (release 9.3) (Gama-Castro et al., 2016).

94 To build our models we randomly selected 80% of the bona fide sRNAs of *R. capsulatus*, *S. pyogenes*  
95 and *S. enterica*. To estimate false positive predictions and build our models, for each bacterial species  
96 we created a set of negative instances by generating random genomic sequences that do not overlap with  
97 the positives instances for the particular bacterium. Basically, negative instances are sets of randomly  
98 selected genomic regions where there is no experimental evidence for the presence of sRNAs. Negative  
99 instances match the length and the strand of the positive instances. To generate the negative instances, we  
100 used BEDTools (Quinlan and Hall, 2010) (code available in Additional File 1). We randomly selected  $n$   
101 negative instances for training, where  $n$  is three times the number of positive instances in the corresponding

102 training set. In previous similar studies,  $n$  has been set to be one (Arnedo et al., 2014) or two (Barman  
103 et al., 2017). However, we believe that a more unbalanced dataset for training is closer to a real scenario,  
104 and decided to increase the value of  $n$  to three. All remaining negative instances were used for validating  
105 the models.

106 An alternative approach to generate negative instances is to take an input sequence and randomly  
107 shuffle the order of its bases as done by Arnedo et al. (2014) and Barman et al. (2017). However, as we use  
108 genomic context features for representing the genomic sequences, shuffling the sequences would preserve  
109 their genomic context properties and therefore be ineffective. Furthermore, as mentioned by Arnedo et al.  
110 (2014) and Lu et al. (2011), the use of non-annotated genomic sequences as negative instances gives a  
111 more conservative estimate of the precision of the models.

112 The number of positive and negative instances per bacterium used for training and validating the  
113 machine learning models is shown in Table 1. Training and validation data are provided in Additional  
114 File 1.

**Table 1.** The number of positive (bona-fide sRNAs) and negative (random genomic sequences) instances in the datasets used for training and validating the classification models. The NCBI accession number of the genome sequence used is indicated in the first column between brackets. The “Combined” data are made by putting together the training data of *S. enterica*, *S. pyogenes* and *R. capsulatus*.

	Training		Validation	
	Positive Instances	Negative Instances	Positive Instances	Negative Instances
<i>R. capsulatus</i> (NC_014034.1)	36	108	9	342
<i>S. pyogenes</i> (NC_002737.2)	37	110	9	349
<i>S. enterica</i> (NC_016810.1)	90	271	23	855
Combined	163	489	N/A	N/A
<i>E. coli</i> (NC_000913.3)	N/A	N/A	125	1245
<i>M. tuberculosis</i> (NC_000962.3)	N/A	N/A	19	190

### 115 sRNA Characterization

116 Each sRNA is represented as a vector of seven numerical features or attributes, as in Gröll et al. (2017).  
117 These attributes are:

- 118 1. free energy of the sRNA predicted secondary structure,
- 119 2. distance to the closest -10 promoter site predicted in the genomic region starting 150 nts upstream  
120 of the start of the sRNA sequence to the end of the sRNA sequence (if no promoter site is predicted  
121 in that region a value of -1000 is used),
- 122 3. distance to the closest predicted Rho-independent terminator in the range of [0,1000] nts (if no  
123 terminator is predicted within this distance range a value of 1000 is used),
- 124 4. distance to the closest left ORF, which is in the range of  $(-\infty, 0]$  nts,
- 125 5. a Boolean value (0 or 1) indicating whether the sRNA is transcribed on the same strand as its left  
126 ORF,
- 127 6. distance to the closest right ORF, which is in the range of  $[0, +\infty)$ , and
- 128 7. a Boolean value indicating whether the sRNA is transcribed on the same strand as its right ORF.

129 A “left” ORF is an annotated ORF located at the 5’ end of a genomic sequence on the forward strand or  
130 located at the 3’ end of a genomic sequence on the reverse strand (Fig.1). A “right” ORF is an annotated  
131 ORF located at the 3’ end of a genomic sequence on the forward strand or located at the 5’ end of a  
132 genomic sequence on the reverse strand.

133 To automatically calculate these seven features for a set of sRNAs from a given bacterial species, we  
134 developed sRNCharP. As input, sRNCharP requires only a BED file (UCSC website, 2018) with the

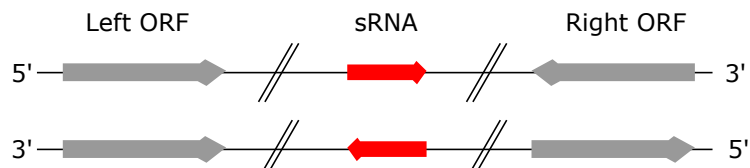


**Figure 1.** Left and right ORFs. Left ORFs are located at the 5' end of an sRNA on the forward strand or at the 3' end of an sRNA on the reverse strand. Right ORFs are located at the 3' end of an sRNA on the forward strand or at the 5' end of an sRNA on the reverse strand.

135 genomic coordinates of the sRNAs, a FASTA file with the corresponding genome sequence, and a BED file  
 136 with the genomic coordinates of the annotated protein coding genes (ORFs). sRNACharP is implemented  
 137 in Nextflow (Di Tommaso et al., 2017) and available at [github.com/BioinformaticsLabAtMUN/](https://github.com/BioinformaticsLabAtMUN/sRNACharP)  
 138 `sRNACharP`. To ensure reproducible results and reduce installation requirements to the minimum,  
 139 sRNACharP is distributed with a Docker container (Di Tommaso et al., 2015). sRNACharP uses the  
 140 following bioinformatics tools (the versions listed within brackets are the ones installed in the Docker  
 141 container). CentroidFold (Hamada et al., 2009) (version 0.0.15) with parameters `-e ``CONTRAFold```  
 142 and `-g 4` is used to predict the secondary structure of the sequences given. BEDtools' `slopBed` and  
 143 `fastaFromBed` (Quinlan and Hall, 2010) (version 2.26) are used to extract the sRNA sequences, and the  
 144 sequences including 150 nts upstream of the 5' end of the sRNAs in FASTA format. Promoter sites  
 145 on the sequences including 150 nts upstream of the 5' end of the sRNAs are predicted using BPROM  
 146 (Solovyev and Salamov, 2011) with default values. Rho-independent terminators are predicted using  
 147 TransTermHP (Kingsford et al., 2007) (version 2.09) with default values. Alternatively, sRNACharP  
 148 can take as input, files from the TransTermHP website ([http://transterm.cbc.umd.edu/](http://transterm.cbc.umd.edu/cgi-bin/transterm/predictions.pl)  
 149 `cgi-bin/transterm/predictions.pl`). For this study, we downloaded the predicted Rho-  
 150 independent terminators for *S. pyogenes* and *M. tuberculosis* from the TransTermHP website on March  
 151 2017. The distances to the closest terminator and the closest ORFs are obtained using BEDtools' `closest`.  
 152 Finally, R (version 3.4.4) is used to generate the features table.

### 153 Machine Learning Approaches

154 We assessed the performance of logistic regression (Cox, 1958; Walker and Duncan, 1967), multilayer  
 155 perceptron (Bishop, 1995; Fahlman, 1988), random forest (Breiman, 2001) and boosting models (Schapire,  
 156 1990) for the task of quantifying the probability of a genomic sequence encoding a bona fide sRNA.  
 157 Random forests and boosting classifiers are both examples of ensemble learning algorithms (Dietterich,  
 158 2000). The core of the boosting methods lies in iteratively combining outputs of so-called “weak learners”,  
 159 converging to an overall strong learner. Logistic regression (LR) was used in Gröll et al. (2017) and  
 160 showed to outperform linear discriminant analysis (LDA) and quadratic discriminant analysis (QDA) for  
 161 this task. We decided to use LR as a baseline to compare the performance of the other classifiers. We  
 162 chose to compare the other four machine learning approaches (classifiers) because they have shown to  
 163 perform well on small datasets and they are generally robust to noise (Liaw and Wiener, 2002; Kerlirzin  
 164 and Vallet, 1993; Ridgeway, 1999).

165 All the machine learning classification approaches were implemented in the Python programming  
 166 language version 3.6. Scikit-learn (version 0.19.1) (Pedregosa et al., 2011) was used for the implemen-  
 167 tation of all the classifiers. For each classifier, the “best” parameters were obtained by optimizing the  
 168 average area under the ROC curve (AUC) when performing leave-one-out cross-validation (LOO CV) on  
 169 the training data (Fig.2).

### 170 Logistic Regression

171 Logistic Regression (LR) learns the parameters  $\beta$  of the logistic function,

$$172 \quad p(X) = \frac{e^{\beta_0 + \beta_1 X_1 + \dots + \beta_n X_n}}{1 + e^{\beta_0 + \beta_1 X_1 + \dots + \beta_n X_n}},$$

173 where  $p(X)$  is the probability of an sRNA with feature vector  $X$  of being a bona fide sRNA,  $e$  is the base  
 174 of the natural logarithm,  $n$  is the number of features, and  $X_i$  is the value of feature  $i$ . To fit the model,  
 175 usually the maximum likelihood approach is used. We used the “balanced” mode that automatically adjust

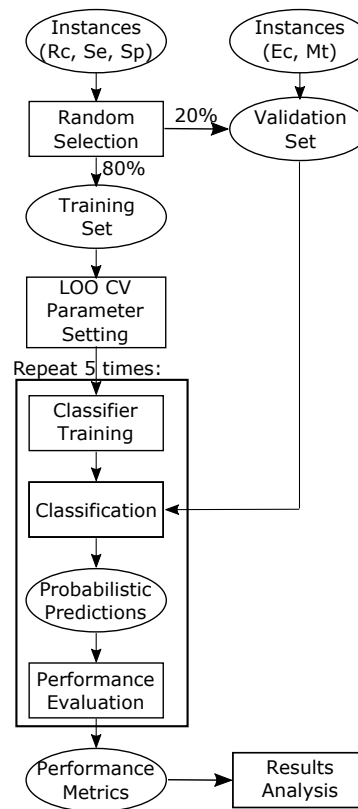


**Figure 2.** Flowchart depicting training and validation methodology. Training and validation datasets are labelled with the corresponding bacterial species: *Ec* = *Escherichia coli*, *Mt* = *Mycobacterium tuberculosis*, *Se* = *Salmonella enterica*, *Sp* = *Streptococcus pyogenes*, and *Rc* = *Rhodobacter capsulatus*.

176 class weights inversely proportional to class frequencies in the input data. All other parameters were left  
 177 to their default values.

### 178 **Multilayer Perceptron**

179 Multilayer Perceptrons (MPs) are fully connected feed-forward neural networks, with one or more layers  
 180 of hidden nodes between the input and output nodes (Bishop, 1995; Fahlman, 1988). Except for the input  
 181 node(s), each node is a neurone with a nonlinear activation function. Each neurone combines weighted  
 182 inputs by computing their sum to determine its output based on a certain threshold value and the activation  
 183 function. The output  $y$  of the system can be described as

$$184 \quad y = f\left(\sum_{i=0}^N w_i x_i\right),$$

185 where  $x_1, \dots, x_N$  represent the input signals,  $w_1, \dots, w_N$  are the synaptic weights and  $f$  is the activation  
 186 function. MPs learn through an iterative process of changing connection weights after processing each  
 187 part of the data. The most common learning algorithm used for this process is backpropagation (Fahlman,  
 188 1988).

189 The activation function that lead to the largest AUCs on the training data was the logistic sigmoid  
 190 function. We used the standard backpropagation algorithm with an initial random generation of weights  
 191  $([-1,1])$ . As using multiple hidden layers decreased the performance, we decided to use only one hidden  
 192 layer. The number of hidden nodes explored was in the range from 1 (in that case the model behaves the  
 193 same as logistic regression) to 1000 with steps of 50. The optimal number of hidden nodes was found to  
 194 be 400. Learning rates ranging from 0.1 to 1.0 were explored in steps of 0.1. The chosen learning rate  
 195 was a constant learning rate of 0.9, because an adaptive learning rate was observed to decrease AUCs.  
 196 The L2 penalty was set to the default value of 0.0001.

### 197 **Random Forest**

198 A random forest (RF) is constructed by combining multiple decision trees during training (Breiman, 2001).  
 199 All decision trees in the random forest contribute to the determination of the final output class. The output  
 200 class is determined by averaging the probabilities produced by the individual trees. The range of number  
 201 of estimators (decision trees) explored was from 1 to 1000 in steps of 100. The optimal setting was found  
 202 to be 400. The largest AUC results were obtained when the nodes are expanded until almost all leaves  
 203 are pure. We tested our model with the maximum depth of the tree ranging from 15 to 25 and found that  
 204 the maximum AUC was obtained at a depth of 20. All features were used in every tree. To measure the  
 205 quality of a split we used the default Gini index (Strobl et al., 2007) and the maximum number of features  
 206 to consider when looking for the best split in a node was set to 2, as calculated by the function tuneRF  
 207 available in the R package randomForest (version 4.6-12).

### 208 **Adaptive Boosting**

209 Adaptive Boosting or AdaBoost (AB) was developed for binary classification problems and tweaks  
 210 “weak learners” by focusing on the instances that were wrongly classified by previous classifiers (Freund  
 211 and Schapire, 1997). Therefore the training error decreases over the iterations. The additive model of  
 212 AdaBoost can be formulated as following. The output of each weak learner is described by:

$$213 \quad L_K(x) = \sum_{k=1}^K l_k(x).$$

214 where  $K$  is the total number of iterations and  $l_k(x)$  is the output function of the weak learner when taking  
 215 the instance  $x$  as input. To minimize the training error  $E_k$  for each iteration  $k$ , AdaBoost uses:

$$216 \quad E_k = \sum_{i=1}^N E(L_{k-1}(x_i) + \alpha_k h(x_i)),$$

217 where  $h(x_i)$  is the predicted output of a weak learner for every instance  $x_i$  in the training set,  $\alpha_k$  is the  
 218 assigned coefficient that minimizes the training error, and  $N$  is the total number of instances in the training  
 219 set.

220 We used AdaBoost on a random forest (RF) classifier that performed just better than chance on the  
 221 training data. The optimal parameters of this RF were found to be 100 decision trees (estimators) and a  
 222 maximum depth of 1. This means all of the trees were decision stumps. The number of estimators was  
 223 established at 100 after exploring a range from 1 to 1000 estimators with steps of 50. A maximum depth  
 224 of 1 was chosen because AdaBoost is known to perform better with decision stumps (Ridgeway, 1999).

### 225 **Gradient Boosting**

226 In gradient boosting (GB) an initial poor fit on the data is improved by fitting base-learners (e.g. decision  
 227 trees) to the negative gradient of a specified loss function (Friedman, 2001). Gradient boosting can be  
 228 described by:

$$229 \quad \hat{f} = \operatorname{argmin}_f E_{x,y}[\rho(Y, f(X))],$$

230 where  $X = \{x_1, \dots, x_n\}$  and  $Y = \{y_1, \dots, y_n\}$ , forming the training set  $\{(x_1, y_1), \dots, (x_n, y_n)\}$ .  $\hat{f}$  minimizes  
 231 expectation  $E$  of the loss function  $\rho$  over all prediction functions  $f$  that take  $X$  as input.

232 We used gradient boosting on 50 estimators (decision trees) with a maximum depth of 15. We  
 233 established the number of estimators by exploring a range of 1 to 1000 estimators with steps of 50. We  
 234 tested our model with the same maximum depth of the tree as for the decision tree classifiers. We then  
 235 gradually decreased the maximum depth taking steps of 1, arriving at 15 as the best setting. The minimum  
 236 number of samples at a leaf node was set to 5, as this was the number found to maximize AUC. Stochastic  
 237 gradient boosting was performed with a subsampling of 0.9.

### 238 **Model Building**

239 As shown in Fig.2 we randomly selected 80% of the positive instances for training, while setting aside the  
 240 other 20% for validating the models. The validation sets were held-out sets used to obtain an unbiased  
 241 estimate of the models performance and were not used to build or fine-tune the models. As the classifiers  
 242 used construct models stochastically, five training runs were carried out for each of the 20 models (five  
 243 machine learning approaches times four training sets) to estimate the stability of the models (script  
 244 available in Additional File 1).

## 245 Performance Assessment

246 Model performance was assessed in terms of the Area Under the Precision-Recall Curve (AUPRC). There  
247 are many classification metrics and none of them can reflect all the strengths and weakness of a classi-  
248 fier (Lever et al., 2016). We have chosen AUPRC as the PRC shows precision values for corresponding  
249 sensitivity (recall) values and is considered more informative than the ROC when evaluating performance  
250 on unbalanced datasets (Saito and Rehmsmeier, 2015). Additionally, precision is a more relevant measure  
251 to many end users, since it represents the proportion of validation experiments for predictions that would  
252 prove successful. We used in-house Python and R scripts to calculate the performance metrics and  
253 generate plots (code is provided in Additional File 1). In Python we used the functions available in  
254 Scikit-learn. In R, we used the packages ROCR (Sing et al., 2005) and PRROC (Grau et al., 2015).

255 Models were evaluated on five validation sets. Each validation set corresponds to data from one  
256 bacterial species. Data of *R. capsulatus*, *S. pyogenes* and *S. enterica* were also used for training, while *E.*  
257 *coli* and *M. tuberculosis* data were used exclusively for validating the models (Table 1). The species for  
258 validation were chosen to be one species of the same taxa as and one of a different taxa from the species  
259 used for training. Median, mean and standard deviation of the performance measurements across the five  
260 training runs were calculated.

261 Additionally, to highlight the difference in performance between the models, we used a “winner-  
262 gets-all” comparison by ranking the methods based on their mean AUPRC for each validation set. The  
263 model(s) with the highest mean AUPRC for a specific validation set were ranked 1 for that validation  
264 set. Ties were all given the same rank. At the end of the ranking process, each model has five ranks  
265 corresponding to one rank per validation set.

266 Analysis of variance (ANOVA) was performed to explore the effects of classifier and training data  
267 on the AUPRC values, and the Tukey’s Honest Significant Difference (HSD) (Tukey, 1949) method was  
268 used to assess the significance on the differences between the mean AUPRC of classifiers, training data,  
269 and models. Additionally, statistical significance of the difference in performance between models was  
270 estimated using the Friedman test which is a non-parametric test recommended for comparison of more  
271 than two classifiers over multiple data sets (Demšar, 2006). To find out which models differ in terms of  
272 performance, we used the Nemenyi post-hoc test (Demšar, 2006), the Quade post-hoc test (García et al.,  
273 2010) and the Conover post-hoc test (Conover, 1999). We used several post-hoc tests as it is recommended  
274 to use several comparison tests (García et al., 2010). All statistical analyses were carried out in R using  
275 the packages PMCMR (Pohlert, 2014) and scmamp (Calvo and Santafe, 2016).

## 276 Attribute Importance

277 To gain insight on how important each attribute is in inferring whether or not a sequence encodes a bona  
278 fide sRNA, we used the function `varImp` available in the R package `randomForest` (version 4.6-12). To  
279 use this function, we first created a RF classifier using the `randomForest` function with `ntree` set  
280 to 400 and `mtry` set to 2. These were the optimal parameters found when tuning the RF classifier (see  
281 above). We generated the RF model using the combined training data (Table 1). Attribute importance was  
282 measured in terms of the mean decrease in accuracy caused by an attribute during the out of bag error  
283 calculation phase of the RF algorithm (Breiman, 2001). The more the accuracy of the RF model decreases  
284 due to the exclusion (or permutation) of a single attribute, the more important that attribute is deemed for  
285 classifying the data.

## 286 Assessing the performance of the best model on benchmark datasets

287 We compared the performance of our best performing model with that of other four existing approaches  
288 as estimated previously by Lu et al. (2011) in a multi-species dataset, and as estimated by Arnedo et al.  
289 (2014) and Barman et al. (2017) in a *Salmonella enterica serovar* Typhimurium LT2 (SLT2) dataset.  
290 We obtained a table with start position, end position, strand and genome of sRNAs in the multi-species  
291 dataset from Lu et al. (2011)’s Supplementary Table S1. We found that 34 sRNAs in Lu et al.’s dataset  
292 were duplicated entries. After removing the duplicated entries we used 754 sRNAs of fourteen different  
293 bacterial species (Table 2). We obtained a table with start position, end position, and name of 182 sRNAs  
294 in the SLT2 dataset from Barman et al. (2017)’s Supplementary Table S6. We noticed that 106 out of the  
295 182 sRNAs in the SLT2 dataset were also contained in Lu et al.’s dataset, and thus the benchmark datasets  
296 are not completely independent. We retrieved the complete genome sequence and genome annotation  
297 of the corresponding bacterium from NCBI. We then extracted the corresponding sRNAs sequences  
298 using BEDtools, and obtained the feature vectors using our sRNACHarP pipeline. We generated the

299 negative instances for each dataset as described above. For Lu et al's dataset, we generated three negative  
 300 instances for each positive instance; however, the ratio of positive to negative instances used by Lu et  
 301 al is not reported in their article and thus the ratio they used may differ from this. For the SLT2 dataset  
 302 we generated ten negative instances for each positive instance to match the ratio of positive to negative  
 303 instances used by Barman et al. (2017).

**Table 2.** Number of positive instances per bacterial species in Lu et al's dataset used in this study. The NCBI accession number of the genome sequence used is indicated in the first column between brackets.

Bacterium	Positive Instances
<i>Burkholderia cenocepacia</i> AU 1054 (NC_008060, NC_008061.1, NC_008062.1)	18
<i>Bacillus subtilis subsp. subtilis</i> str. 168 (NC_000964.3)	12
<i>Caulobacter crescentus</i> CB15 (NC_002696.2)	7
<i>Chlamydia trachomatis</i> L2b/UCH-1/proctitis (NC_010280.2)	23
<i>Escherichia coli</i> K12 MG1655 (NC_000913.3)	79
<i>Helicobacter pylori</i> 26695 (NC_000915.1)	50
<i>Listeria monocytogenes</i> EGD-e (NC_003210.1)	56
<i>Pseudomonas aeruginosa</i> PA01 (NC_002516.2)	17
<i>Staphylococcus aureus subsp. aureus</i> N315 (NC_002745.2)	9
<i>Streptomyces coelicolor</i> A3(2) (NC_003888.3)	3
<i>Salmonella enterica subsp. enterica serovar</i> Typhimurium str. LT2 (NC_003197.2)	115
<i>Shewanella oneidensis</i> MR-1 (NC_004347.2)	9
<i>Vibrio cholerae</i> O1 biovar El Tor str. N16961 (NC_002505.1, NC_002506.1)	137
<i>Xenorhabdus nematophila</i> ATCC 19061 (NC_014228.1)	219

## 304 RESULTS

### 305 Performance Assessment

306 In this section models are identified by the classifier and the training data used. Training and validation  
 307 datasets are labelled with the corresponding bacterial species: Ec = *Escherichia coli*, Mt = *Mycobacterium*  
 308 *tuberculosis*, Se = *Salmonella enterica*, Sp = *Streptococcus pyogenes*, and Rc = *Rhodobacter capsulatus*.  
 309 The distribution of AUPRC for each classifier is shown in Fig. 3. As LR was clearly outperformed by the  
 310 other four classifiers, we excluded LR results from further analysis.

311 The mean AUPRC for each of the 16 models is depicted in Fig. 4. For the four classifiers, models  
 312 trained on the Rc training data have lower AUPRC values than models trained on the other three training  
 313 sets. The classifier producing the most variable models was MP with average standard deviations above  
 314 the overall mean standard deviation; while AB was the classifier with the lowest standard deviation.  
 315 AB is the classifier least susceptible to variations in AUPRC due to the training data; while, MP is the  
 316 classifier with more variation in AUPRC due to the training data (Fig. 4). ANOVA results indicated  
 317 that the classifier and the training data are both significant factors to explain variance in AUPRC values  
 318 (F-statistic = 8.29, p-value  $2.34e^{-5}$  and F-statistic = 8.26, p-value  $2.46e^{-5}$ , respectively). There was not  
 319 significant interaction between these two factors found by ANOVA.

320 To emphasize differences in performance among the models, we ranked each model based on mean  
 321 AUPRC obtained on each validation set (see Methods). The model with the highest AUPRC is ranked  
 322 one, and ties are assigned the same rank. Fig. 5 depicts the mean rank of each classifier. The Friedman  
 323 test (pvalue = 0.008) indicated that the average rank obtained by some of the classifiers is significantly  
 324 different from the mean rank expected under the null hypothesis. We then used three post-hoc tests for  
 325 pairwise comparisons. The Nemenyi test identified two groups of classifiers with similar ranks: RF, AB  
 326 and GB in one group, and AB, GB and MP in the other group. According to the Nemenyi test, the ranks  
 327 of RF are statistically significantly lower (pvalue = 0.008) than the ranks of MP (Fig. 6). The Quade  
 328 post-hoc test deemed the differences in ranks between RF and MP (FDR corrected pvalue = 0.002) and  
 329 between RF and GB (FDR corrected pvalue = 0.006) as statistically significant. Finally, the Conover  
 330 post-hoc test found statistically significant differences between the ranks of RF vs MP (FDR corrected  
 331 pvalue = 0.0005), RF vs GB (FDR corrected pvalue = 0.002), RF vs AB (FDR corrected pvalue = 0.018),

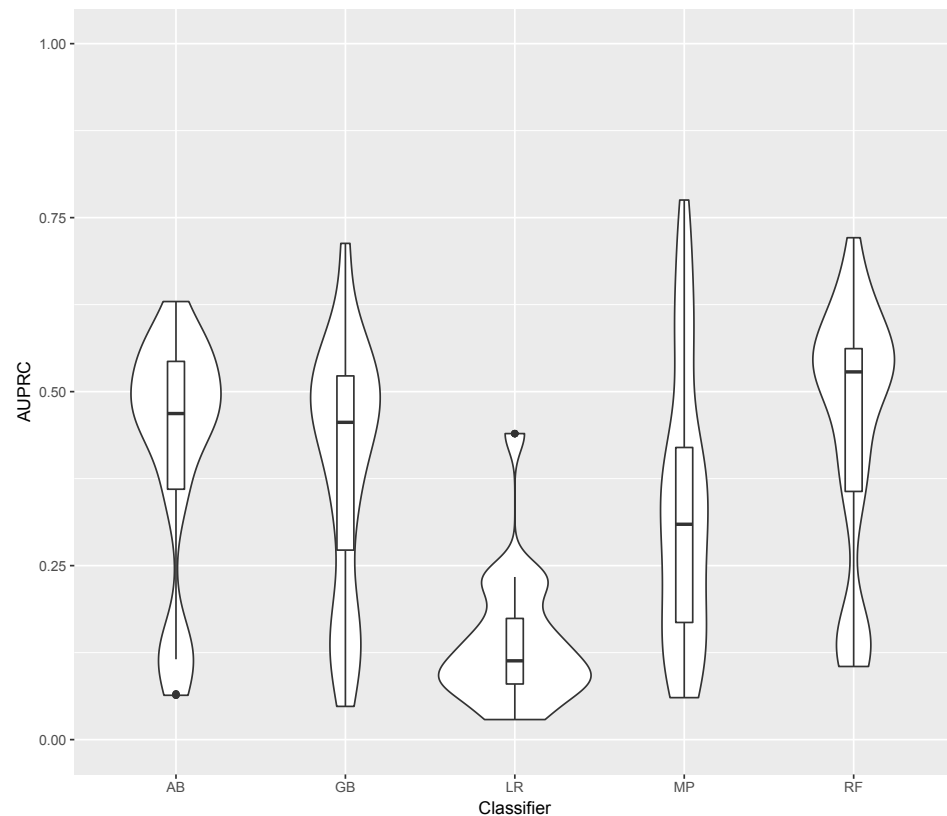


**Figure 3.** Distribution of AUPRC values per classifier. Violin plots illustrate the distribution of AUPRC values for all models obtained with each classifier. Inside the distribution shape a box indicates the range from the 25 percentile to 75 percentile of the precision values. AB = Adaptive Boosting, GB = Gradient Boosting, LR = Logistic Regression, MP = Multilayer Perceptron, RF = Random Forest.

332 and AB vs MP (FDR corrected pvalue = 0.031). Based on these results, we concluded that RF is the only  
 333 classifier with significant differences in ranks with respect to the other classifiers. We selected the RF -  
 334 Combined model as our best performing model, as it has one of the highest mean AUPRC, lowest mean  
 335 rank and low standard deviation. However, these three models: RF-Combined, RF-Sp and RF-Se are  
 336 likely comparable in terms of mean rank and AUPRC (Fig. 4 and Additional Fig. 1).

337 To facilitate other researchers to rank their own sRNAs, we have created sRNARanking, an R  
 338 script that produces the probabilistic predictions generated by the RF-Combined model. We used R  
 339 to distribute the model because R is more commonly used by natural science researchers than Python.  
 340 sRNARanking takes as input the feature table produced by sRNACHarP and calculates the probability  
 341 of being a bona fide sRNA for each sRNA included in the feature table. sRNARanking is available at  
 342 <https://github.com/BioinformaticsLabAtMUN/sRNARanking>.

### 343 Attribute Importance

344 Based on the mean decrease in accuracy estimated by the random forest algorithm, all attributes contribute  
 345 positively to obtain a more accurate model (Fig. 7). The seven attributes clustered in three levels of  
 346 importance: those with a mean decrease in accuracy greater than 20; those with a mean decrease in  
 347 accuracy between 10 and 15, and those with a mean decrease in accuracy lower than 10. The most  
 348 important attributes are the distance to the closest ORFs and the distance to the closest predicted Rho-  
 349 independent terminator. The two attributes that seem to contribute the least to the accuracy of a model are  
 350 the Boolean features indicating whether or not a genomic sequence is transcribed on the same strand as  
 351 its closest ORFs.

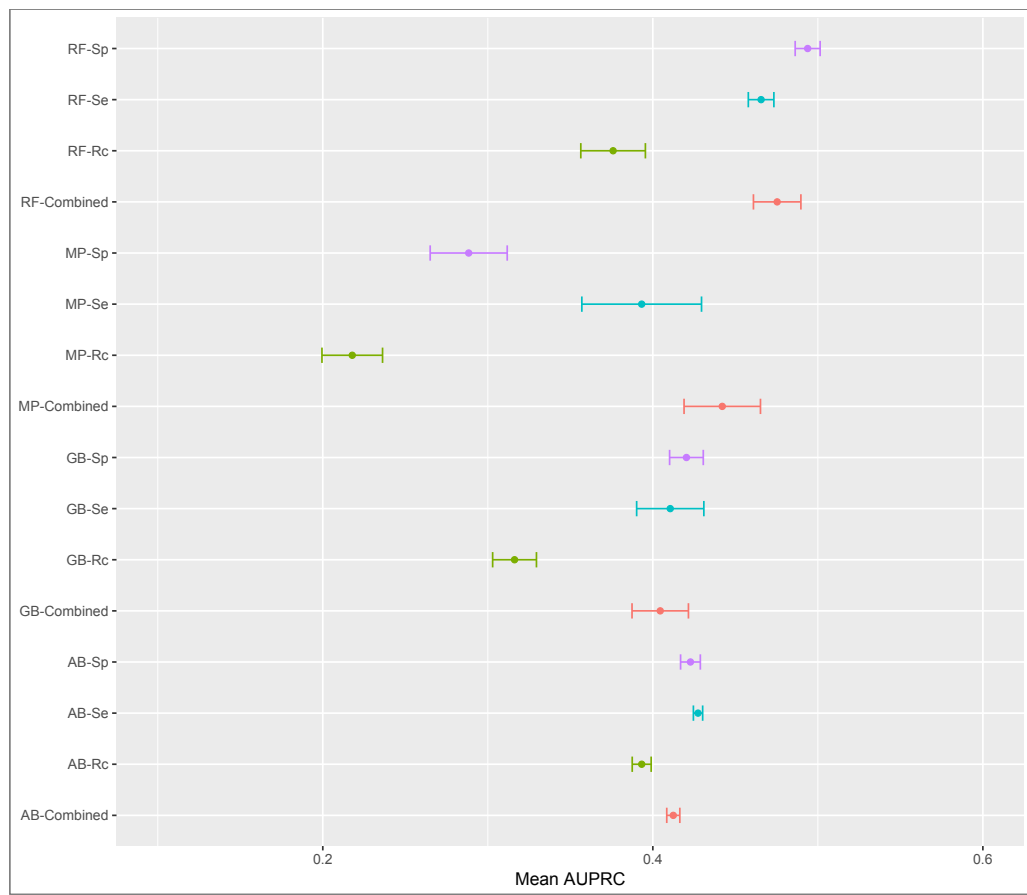


**Figure 4.** Mean AUPRC per model. The dot represents the mean AUPRC and bars represent standard error. Colour indicates the training data used: Red = Combined data, Green = *R. capsulatus* data, Blue = *S. enterica* data, Purple = *S. pyogenes* data. Classifiers are indicated by AB = Adaptive Boosting, GB = Gradient Boosting, MP = Multilayer Perceptron, RF = Random Forest.

### 352 Assessing the performance of our best model on benchmark datasets

353 Lu et al. (2011) evaluated the performance of four comparative genomics-based leading tools for sRNA  
 354 prediction on a dataset composed of sRNAs from 14 different bacteria (Table 2), and found recall rates  
 355 of 20% - 49% with precisions of 6%-12%; while our RF-combined model (sRNARanking) achieved  
 356 precision rates of 85% to 96% at those same recall rates (Fig. 8).

357 Arnedo et al. (2014) and Barman et al. (2017) evaluated the performance of their methods in terms of  
 358 sensitivity (recall) and specificity. Fig. 9 top shows the Sensitivity-Specificity curve of sRNARanking on  
 359 the SLT2 dataset. At a sensitivity of 67%, Arnedo et al's approach has a specificity of 78% (Barman et al.,  
 360 2017), while sRNARanking at the same sensitivity level has a specificity of 94% and a precision of 54%  
 361 (Fig. 9 bottom). sRNARanking's specificity of 88% is comparable to the 91% specificity of Barman et  
 362 al's approach at a sensitivity of 85%.

363 The main goal of this study was to precisely rank sRNAs detected from RNA-seq data to guide further  
 364 experiments to functionally characterize sRNAs. If we assume that microbiologists would only select a  
 365 few of the top-scoring predictions for Northern blot validation, then at a sensitivity (recall) level of 10%,  
 366 sRNARanking has a precision of 90% on the SLT2 dataset (Fig. 9 bottom). In other words, if we assume  
 367 that the top 10% predictions would be selected for Northern blot validation, only two out of 18 candidate  
 368 sRNAs would fail to be detected.

## 369 DISCUSSION

370 We anticipated that the distance to the closest promoter, the distance to the closest terminator and the  
 371 energy of the secondary structure would be the most important attributes to predict whether or not a

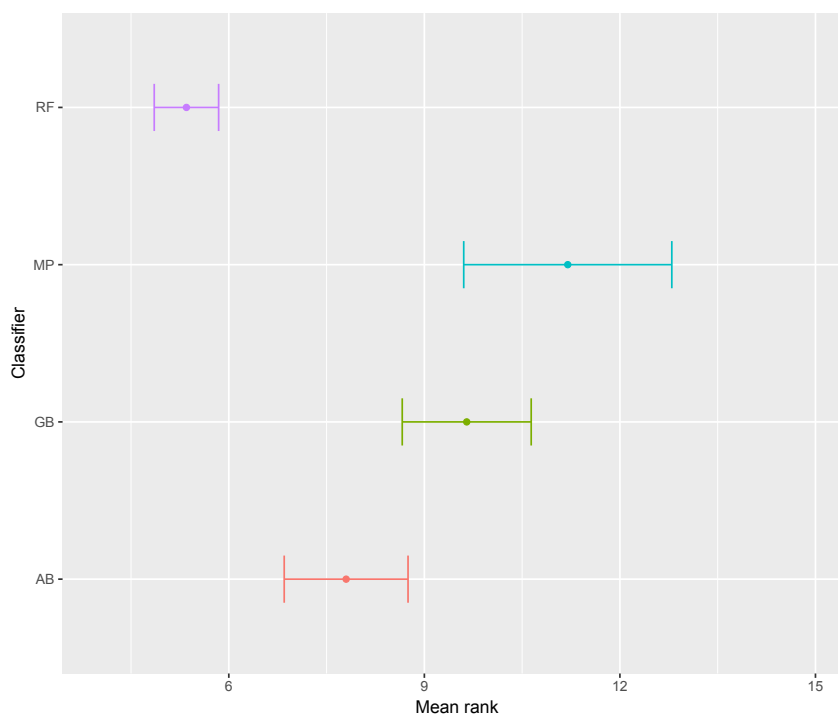


**Figure 5.** Mean rank per classifier. The dot represents the mean rank and bars represent standard error. Lower ranks indicate better performance in terms of AUPRC. Classifiers are indicated by AB = Adaptive Boosting, GB = Gradient Boosting, MP = Multilayer Perceptron, RF = Random Forest.

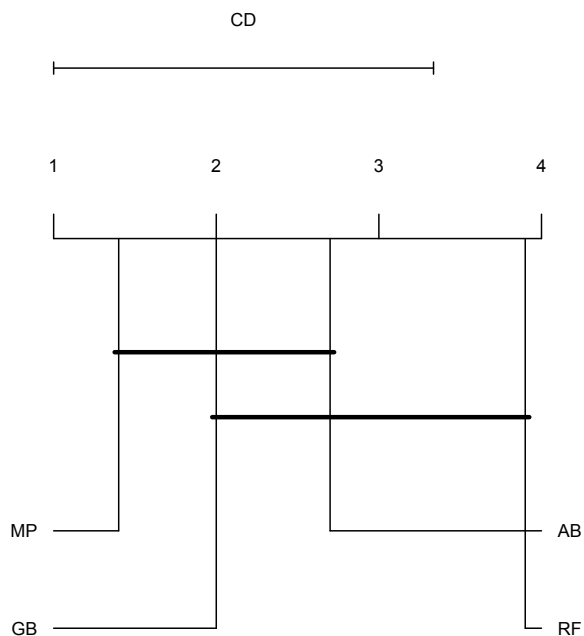


**Figure 6.** Critical difference plot. Classifiers that are not deemed significantly different by the Nemenyi test at a significance level of 0.05 are connected.

372 genomic sequence is a bona fide sRNA. As promoters determine when and how transcription of a nearby  
 373 gene is initiated, we expected genuine sRNAs to be close to a promoter. However, as current best

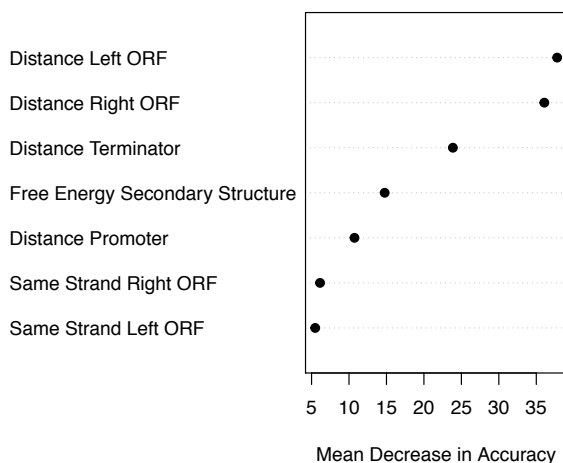


**Figure 7.** Attribute importance. Mean decrease in accuracy per attribute as estimated by the random forest algorithm. Attribute importance is plotted on the x-axis. Attributes are ordered top-to-bottom as most- to least-important. Three levels of importance are observed: high importance attributes (distances to closest ORFs and distance to terminator); medium importance attributes (free energy of secondary structure and distance to promoter), and low importance attributes (same strandness as closest ORFs).

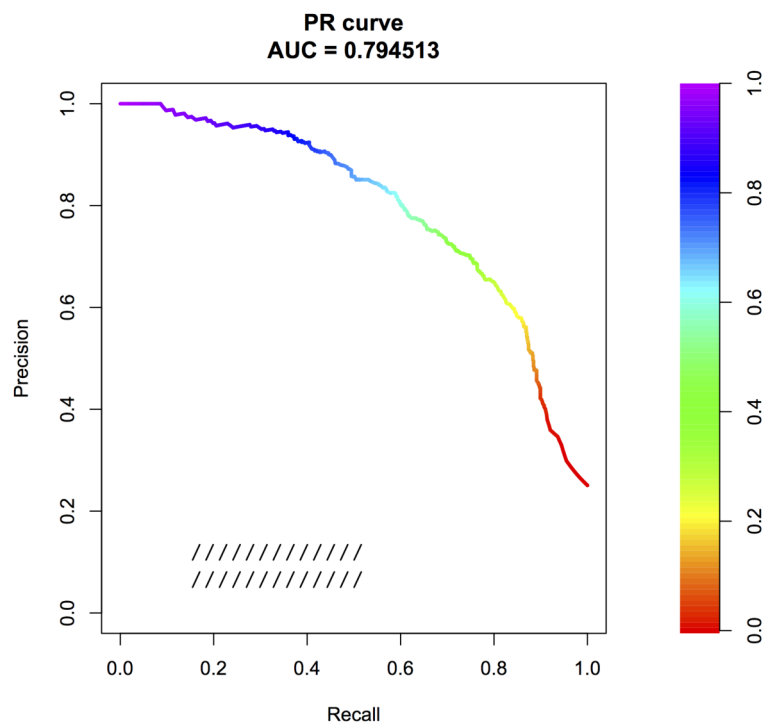


**Figure 8.** PRC of sRNARanking performance on Lu et al's multi-species dataset. The four approaches assessed by Lu et al achieved recall of 0.20 to 0.49 with precision of 0.06 to 0.12. The corresponding area in the PRC is indicated by forward slashes. The colour scale on the left indicates probability thresholds yielding the points on the curve.

374 programs to predict promoters have a recall rate between 49% and 59% (Shahmuradov et al., 2017), many  
 375 sRNAs might incorrectly be represented as not having a promoter nearby when in fact they do. Gene  
 376 expression in bacteria is also regulated by termination of transcription, often in response to specific signals.

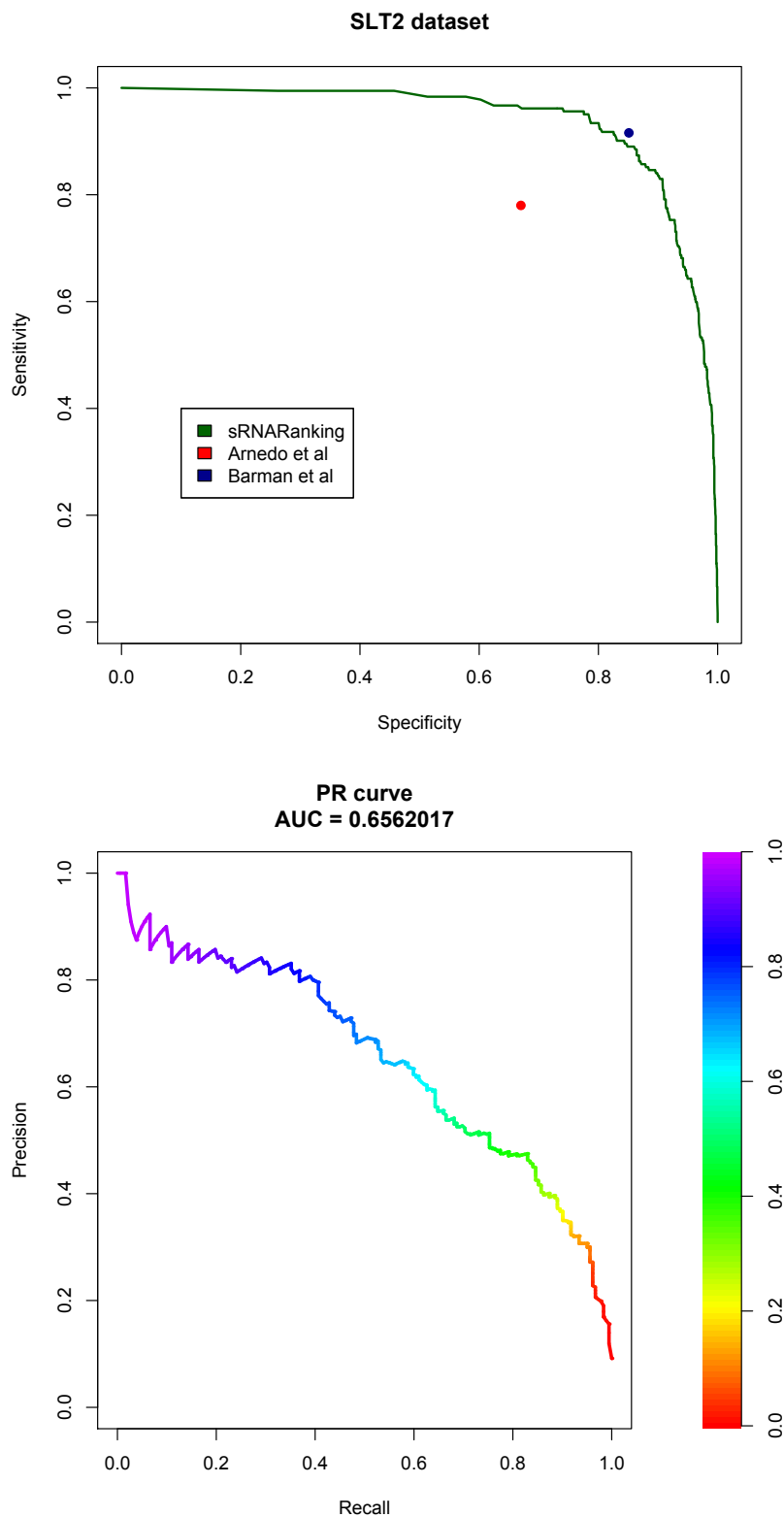


**Figure 9.** sRNARanking performance on the SLT2 dataset. Top: Sensitivity-Specificity curve of sRNARanking performance. Arnedo et al's approach and Barman et al's approach reported sensitivity and specificity are indicated with a red and a blue dot, respectively. Bottom: Precision-Recall curve of sRNARanking performance on the SLT2 dataset. The colour scale on the left indicates probability thresholds yielding the points on the curve.

377 Being in proximity to a Rho-independent terminator is often used as evidence for genome annotation.  
378 However, bacteria commonly regulate gene expression by using *cis*-acting RNA elements for conditional  
379 transcription termination. These *cis*-acting terminators are not predicted by TransTermHP, and thus many  
380 sRNAs might incorrectly be represented as not being in the proximity to a terminator. We expect that  
381 improving bacterial promoter and terminator prediction will increase the importance of these features  
382 and improve sRNA prediction using genomic context features. Many sRNAs have a stable secondary  
383 structure; however, sRNAs are also known to show heterogeneous structures (Wagner and Romby, 2015).  
384 This might reduce the importance of the energy of the secondary structure as a feature to predict sRNAs.  
385 We believe that the distances to the closest ORFs are the most important attributes partially due to a bias  
386 in the training data. 93% of the negative instances (random genomic sequences) in the combined training  
387 data overlap the two neighbouring ORFs (i.e., their distances to their closest ORFs are zero), while 70%  
388 of the positive instances (bona fide sRNAs) are intergenic (i.e., their absolute distances to their closest  
389 ORFs are greater than zero). This bias in the data may be corrected as more antisense sRNAs (asRNAs)  
390 and partially overlapping sRNAs are experimentally verified as bona fide sRNAs.

391 We hypothesized that *R. capsulatus* training data produced worse performing models because it  
392 includes as positive instances a higher number of non-intergenic sRNAs (18 or 50%). In fact, the best  
393 performing model obtained lower AUPRC for *R. capsulatus* and *E. coli* validation datasets (Additional  
394 Figs. 2-6). These two bacterial species have the higher proportion of non-intergenic bona fide sRNAs:  
395 51% and 40% of the bona fide sRNAs of *R. capsulatus* and *E. coli*, respectively, overlap neighbouring  
396 ORFs; while 17.4%, 26.5% and 36.8% of the bona fide sRNAs of *S. pyogenes*, *S. enterica* and *M.*  
397 *tuberculosis*, respectively, overlap neighbouring ORFs. Additionally, 17 *R. capsulatus* putative sRNAs  
398 included as positive instances were found to be conserved in the genome of at least two other bacterial  
399 species but have not been verified in the wet lab. Some of these 17 putative *R. capsulatus* sRNAs chosen  
400 as positive instances based on sequence conservation may actually be false positives. Barman et al. (2017)  
401 also observed that the performance of their approach for predicting *E. coli* sRNAs was inferior than the  
402 performance obtained for other bacteria. They suggested that a reason for this might be the higher number  
403 of experimentally verified sRNAs of *E. coli* overlapping with ORFs (Barman et al., 2017).

404 With respect to the different machine learning approaches assessed, RF seems to be better suited for  
405 the task of prioritizing bona fide sRNAs than the other four classifiers (AB, GB, MP and LR). Statistical  
406 tests results supported this by deeming the difference in performance between the models obtained by RF  
407 and models obtained by the other classifiers as statistically significant. To be able to use deep learning for  
408 sRNA prioritization, datasets at least one order of magnitude larger than the ones currently available are  
409 required.

410 To demonstrate the ability of the models to generalize to other bacterial species, we validated the  
411 models on data from bacterial species that were not part of the training set. In fact, using data from the  
412 same bacterial species on the training and validation sets was not a factor to explain variance in model  
413 performance. This indicates that models are able to learn sRNAs features that are species independent, and  
414 even taxa independent as the AUPRC values obtained in the *M. tuberculosis* validation set suggest. Using  
415 data from different bacterial species and experimental conditions is expected to lead to improved predictive  
416 models. In fact, training the classifiers with the combined data generated models that either outperform, or  
417 were comparable to, the models obtained from training the classifiers with data from a single bacterium.  
418 To allow other researchers to rank their own sRNAs, we have implemented sRNARanking, an R script  
419 containing the RF-Combined model.

420 To compare our best performing model with current approaches, we evaluated sRNARanking on a  
421 multi-species dataset (Lu et al., 2011) and demonstrated that sRNARanking clearly outperformed four  
422 comparative genomics-based approaches in terms of precision rates (85% to 96% vs 6% to 12%) at the  
423 same recall rates (Fig. 8). Additionally, we compared sRNARanking performance on a SLT2 dataset  
424 with two more recently published approaches: a meta-approach (Arnedo et al., 2014) and a SVM-based  
425 approach (Barman et al., 2017). sRNARanking achieved better performance than the meta-approach and  
426 comparable performance to the SVM-based approach in terms of sensitivity and specificity (Fig. 9).

427 A multitude of sRNAs have been detected in many bacterial species. The sheer number of novel  
428 putative sRNAs reported in the literature makes it infeasible to validate in the web lab each of them.  
429 Thus, there is the need for computational approaches to characterize putative sRNAs and to rank these  
430 sRNAs on the basis of their likelihood of being bona fide sRNAs. Our results demonstrate that a RF-based  
431 approach using genomic context and structure-based features is able to detect intrinsic features of sRNAs

432 common to a number of bacterial species, overcoming the challenge of the low sequence conservation of  
433 sRNAs. As the number of detected sRNAs continues to raise, computational predictive models as the one  
434 here generated will become increasingly valuable to guide further investigations.

## 435 ABBREVIATIONS

436 LR: logistic regression; MP: multilayer perceptron; AB: adaptive boosting; GB: gradient boosting; RF:  
437 random forest; FDR: false discovery rate; AUC: area under receiver operating characteristic curve;  
438 AUPRC: area under the precision-recall curve; LOO CV: leave-one-out cross-validation; ORF: open  
439 reading frame; nts: nucleotides; sRNA: small non-coding RNA.

## 440 ACKNOWLEDGEMENTS

441 We thank Emilio Palumbo for providing technical support for the implementation in Nextflow, and Dr.  
442 Meruvia-Pastor for providing feedback on the manuscript.

## 443 REFERENCES

- 444 Arnedo, J., Romero-Zaliz, R., Zwir, I., and Del Val, C. (2014). A multiobjective method for robust  
445 identification of bacterial small non-coding RNAs. *Bioinformatics*, 30(20):2875–82.
- 446 Backofen, R. and Hess, W. R. (2010). Computational prediction of sRNAs and their targets in bacteria.  
447 *RNA Biol*, 7(1):33–42.
- 448 Barman, R. K., Mukhopadhyay, A., and Das, S. (2017). An improved method for identification of small  
449 non-coding RNAs in bacteria using support vector machine. *Sci Rep*, 7:46070.
- 450 Bishop, C. M. (1995). Neural networks for pattern recognition. *Oxford university press.*, 3rd ed.
- 451 Breiman, L. (2001). Random forests. *Machine Learning*, 45(1):5–32.
- 452 Calvo, B. and Santafe, G. (2016). scmamp: Statistical comparison of multiple algorithms in multiple  
453 problems. *The R Journal*, 8(1).
- 454 Conover, W. (1999). *Practical Nonparametric Statistics*. John Wiley & Sons, 3rd edition.
- 455 Cox, D. R. (1958). The regression analysis of binary sequences. *Journal of the Royal Statistical Society*  
456 *Series B (Methodological)*, pages 215–242.
- 457 Demšar, J. (2006). Statistical comparisons of classifiers over multiple data sets. *J. Mach. Learn. Res.*,  
458 7:1–30.
- 459 Di Tommaso, P., Chatzou, M., Floden, E. W., Barja, P. P., Palumbo, E., and Notredame, C. (2017).  
460 Nextflow enables reproducible computational workflows. *Nat Biotechnol*, 35(4):316–319.
- 461 Di Tommaso, P., Palumbo, E., Chatzou, M., Prieto, P., Heuer, M. L., and Notredame, C. (2015). The  
462 impact of docker containers on the performance of genomic pipelines. *PeerJ*, 3:e1273.
- 463 Dietterich, T. G. (2000). Ensemble methods in machine learning. *Multiple classifier systems*, 1857:1–15.
- 464 Fahlman, S. E. (1988). Faster-learning variations on backpropagation: An empirical study. *Proceedings*  
465 *of the Connectionist Models Summer School*, pages 38–51.
- 466 Freund, Y. and Schapire, R. (1997). A decision-theoretic generalization of on-line learning and an  
467 application to boosting. *Journal of Computer and System Sciences*, 55(1):119 – 139.
- 468 Friedman, J. H. (2001). Greedy function approximation: A gradient boosting machine. *The Annals of*  
469 *Statistics*, 29(5):1189–1232.
- 470 Gama-Castro, S., Salgado, H., Santos-Zavaleta, A., Ledezma-Tejeida, D., Muñoz-Rascado, L., García-  
471 Sotelo, J. S., Alquicira-Hernández, K., Martínez-Flores, I., Pannier, L., Castro-Mondragón, J. A.,  
472 Medina-Rivera, A., Solano-Lira, H., Bonavides-Martínez, C., Pérez-Rueda, E., Alquicira-Hernández,  
473 S., Porrón-Sotelo, L., López-Fuentes, A., Hernández-Koutoucheva, A., Del Moral-Chávez, V., Rinaldi,  
474 F., and Collado-Vides, J. (2016). RegulonDB version 9.0: high-level integration of gene regulation,  
475 coexpression, motif clustering and beyond. *Nucleic Acids Res*, 44(D1):D133–43.
- 476 García, S., Fernández, A., Luengo, J., and Herrera, F. (2010). Advanced nonparametric tests for multiple  
477 comparisons in the design of experiments in computational intelligence and data mining: Experimental  
478 analysis of power. *Inf. Sci.*, 180(10):2044–2064.
- 479 Grau, J., Grosse, I., and Keilwagen, J. (2015). PRROC: computing and visualizing precision-recall and  
480 receiver operating characteristic curves in R. *Bioinformatics*, 31(15):2595–7.

- 481 Grüll, M. P., Peña-Castillo, L., Mulligan, M. E., and Lang, A. S. (2017). Genome-wide identification and  
482 characterization of small RNAs in *Rhodobacter capsulatus* and identification of small RNAs affected  
483 by loss of the response regulator CtrA. *RNA Biol*, pages 1–12.
- 484 Hamada, M., Kiryu, H., Sato, K., Mituyama, T., and Asai, K. (2009). Prediction of RNA secondary  
485 structure using generalized centroid estimators. *Bioinformatics (Oxford, England)*, 25(4):465–473.
- 486 Kerlirzin, P. and Vallet, F. (1993). Robustness in multilayer perceptrons. *Neural computation*, 5(3):473–  
487 482.
- 488 Kingsford, C. L., Ayanbule, K., and Salzberg, S. L. (2007). Rapid, accurate, computational discovery of  
489 Rho-independent transcription terminators illuminates their relationship to DNA uptake. *Genome Biol*,  
490 8(2):R22.
- 491 Kröger, C., Dillon, S. C., Cameron, A. D. S., Papenfort, K., Sivasankaran, S. K., Hokamp, K., Chao, Y.,  
492 Sittka, A., Hébrard, M., Händler, K., Colgan, A., Leekitcharoenphon, P., Langridge, G. C., Lohan, A. J.,  
493 Loftus, B., Lucchini, S., Ussery, D. W., Dorman, C. J., Thomson, N. R., Vogel, J., and Hinton, J. C. D.  
494 (2012). The transcriptional landscape and small RNAs of *Salmonella enterica* serovar typhimurium.  
495 *Proc Natl Acad Sci U S A*, 109(20):E1277–86.
- 496 Le Rhun, A., Beer, Y. Y., Reimegård, J., Chylinski, K., and Charpentier, E. (2016). RNA sequencing  
497 uncovers antisense RNAs and novel small RNAs in *Streptococcus pyogenes*. *RNA Biol*, 13(2):177–95.
- 498 Lever, J., Krzywinski, M., and Altman, N. (2016). Classification evaluation. *Nature Methods*, 13:603–604.
- 499 Liaw, A. and Wiener, M. (2002). Classification and regression by randomForest. *R news*, 2(3):18–22.
- 500 Lu, X., Goodrich-Blair, H., and Tjaden, B. (2011). Assessing computational tools for the discovery of  
501 small RNA genes in bacteria. *RNA*, 17(9):1635–47.
- 502 McClure, R., Tjaden, B., and Genco, C. (2014). Identification of sRNAs expressed by the human pathogen  
503 *Neisseria gonorrhoeae* under disparate growth conditions. *Frontiers in microbiology*, 5:456.
- 504 Michaux, C., Verneuil, N., Hartke, A., and Giard, J.-C. (2014). Physiological roles of small RNA  
505 molecules. *Microbiology*, 160(Pt 6):1007–19.
- 506 Miotto, P., Forti, F., Ambrosi, A., Pellin, D., Veiga, D. F., Balazsi, G., Gennaro, M. L., Di Serio, C.,  
507 Ghisotti, D., and Cirillo, D. M. (2012). Genome-wide discovery of small RNAs in *Mycobacterium*  
508 *tuberculosis*. *PLoS One*, 7(12):e51950.
- 509 Pedregosa, F., Varoquaux, G., Gramfort, A., Michel, V., Thirion, B., Grisel, O., Blondel, M., Prettenhofer,  
510 P., Weiss, R., Dubourg, V., Vanderplas, J., Passos, A., Cournapeau, D., Brucher, M., Perrot, M., and  
511 Duchesnay, E. (2011). Scikit-learn: Machine learning in Python. *Journal of Machine Learning*  
512 *Research*, 12:2825–2830.
- 513 Pohlert, T. (2014). *The Pairwise Multiple Comparison of Mean Ranks Package (PMCMR)*. R package.
- 514 Quinlan, A. R. and Hall, I. M. (2010). BEDTools: a flexible suite of utilities for comparing genomic  
515 features. *Bioinformatics*, 26(6):841–2.
- 516 Ridgeway, G. (1999). The state of boosting. *Computing Science and Statistics*, pages 172–181.
- 517 Saito, T. and Rehmsmeier, M. (2015). The precision-recall plot is more informative than the ROC plot  
518 when evaluating binary classifiers on imbalanced datasets. *PLoS One*, 10(3):e0118432.
- 519 Schapire, R. E. (1990). The strength of weak learnability. *Machine Learning*, 5(2):197–227.
- 520 Shahmuradov, I. A., Mohamad Razali, R., Bougouffa, S., Radovanovic, A., and Bajic, V. B. (2017).  
521 bTSSfinder: a novel tool for the prediction of promoters in *cyanobacteria* and *Escherichia coli*.  
522 *Bioinformatics*, 33(3):334–340.
- 523 Sing, T., Sander, O., Beerenwinkel, N., and Lengauer, T. (2005). ROCr: visualizing classifier performance  
524 in R. *Bioinformatics*, 21(20):3940–1.
- 525 Solovyev, V. V. and Salamov, A. (2011). Automatic annotation of microbial genomes and metagenomic  
526 sequences. *Metagenomics and its Applications in Agriculture, Biomedicine and Environmental Studies*.
- 527 Soutourina, O. A., Monot, M., Boudry, P., Saujet, L., Pichon, C., Sismeiro, O., Semenova, E., Severinov,  
528 K., Le Bouguenec, C., Coppée, J.-Y., Dupuy, B., and Martin-Verstraete, I. (2013). Genome-wide identi-  
529 fication of regulatory RNAs in the human pathogen *Clostridium difficile*. *PLoS Genet*, 9(5):e1003493.
- 530 Storz, G., Vogel, J., and Wassarman, K. M. (2011). Regulation by small RNAs in bacteria: expanding  
531 frontiers. *Mol Cell*, 43(6):880–91.
- 532 Strobl, C., Boulesteix, A. L., and Augustin, T. (2007). Unbiased split selection for classification trees  
533 based on the Gini index. *Computational Statistics and Data Analysis*, 52(1):483–501.
- 534 Thomason, M. K., Bischler, T., Eisenbart, S. K., Forstner, K. U., Zhang, A., Herbig, A., Nieselt, K.,  
535 Sharma, C. M., and Storz, G. (2015). Global transcriptional start site mapping using differential RNA

- 536 sequencing reveals novel antisense RNAs in *Escherichia coli*. *Journal of Bacteriology*, 197(1):18–28.
- 537 Tukey, J. W. (1949). Comparing individual means in the analysis of variance. *Biometrics*, 5(2):99–114.
- 538 UCSC website (2018). BED format description.
- 539 Vockenhuber, M.-P., Sharma, C. M., Statt, M. G., Schmidt, D., Xu, Z., Dietrich, S., Liesegang, H.,  
540 Mathews, D. H., and Suess, B. (2011). Deep sequencing-based identification of small non-coding  
541 RNAs in *Streptomyces coelicolor*. *RNA Biol*, 8(3):468–77.
- 542 Wagner, E. G. H. and Romby, P. (2015). Small RNAs in bacteria and archaea: who they are, what they do,  
543 and how they do it. *Adv Genet*, 90:133–208.
- 544 Walker, S. H. and Duncan, D. B. (1967). Estimation of the probability of an event as a function of several  
545 independent variables. *Biometrika*, 54(1-2):167–179.
- 546 Wilms, I., Overlöper, A., Nowrousian, M., Sharma, C. M., and Narberhaus, F. (2012). Deep sequencing  
547 uncovers numerous small RNAs on all four replicons of the plant pathogen *Agrobacterium tumefaciens*.  
548 *RNA Biol*, 9(4):446–57.
- 549 Zeng, Q. and Sundin, G. W. (2014). Genome-wide identification of Hfq-regulated small RNAs in the fire  
550 blight pathogen *Erwinia amylovora* discovered small RNAs with virulence regulatory function. *BMC*  
551 *genomics*, 15:414–2164–15–414.